

Label Semantic Knowledge Distillation for Unbiased Scene Graph Generation

Lin Li, Long Chen*, Hanrong Shi, Wenxiao Wang, Jian Shao, Yi Yang, Jun Xiao

Abstract—The Scene Graph Generation (SGG) task aims to detect all the objects and their pairwise visual relationships in a given image. Although SGG has achieved remarkable progress over the last few years, almost all existing SGG models follow the same training paradigm: they treat both object and predicate classification in SGG as a single-label classification problem, and the ground-truths are one-hot target labels. However, this prevalent training paradigm has overlooked two characteristics of current SGG datasets: 1) For positive samples, some specific subject-object instances may have multiple reasonable predicates. 2) For negative samples, there are numerous missing annotations. Regardless of the two characteristics, SGG models are easy to be confused and make wrong predictions. To this end, we propose a novel model-agnostic Label Semantic Knowledge Distillation (LS-KD) for unbiased SGG. Specifically, LS-KD dynamically generates a “soft” label for each subject-object instance by fusing a predicted Label Semantic Distribution (LSD) with its original one-hot target label. LSD reflects the correlations between this instance and multiple predicate categories. Meanwhile, we propose two different strategies to predict LSD: iterative self-KD and synchronous self-KD. Extensive ablations and results on three SGG tasks have attested to the superiority and generality of our proposed LS-KD, which can consistently achieve decent trade-off performance between different predicate categories.

Index Terms—Unbiased Scene Graph Generation, Knowledge Distillation

I. INTRODUCTION

Scene Graph Generation (SGG), *i.e.*, detecting all the objects (including both localization and classification) and classifying their pairwise visual relationships in a given image, is a challenging and fundamental scene understanding task [1]. Typically, a scene graph can be formulated as a series of subject-predicate-object triplets (*e.g.*, “man-on-chair” in Fig. 1(a)). Due to its symbolic representation nature, SGG has played an important role in many downstream tasks, such as image captioning [2], [3], [4], [5], [6], image retrieval [7], [8], visual question answering [9], [10], [11], and so on. Meanwhile, with the release of several large-scale SGG datasets (*e.g.*, Visual Genome (VG) [12]) and the maturity of advanced object detectors [13], SGG has raised unprecedented attention over the recent few years, and hundreds of SGG models have been proposed [14], [15], [16], [17].

However, one notorious challenge in existing SGG benchmarks is the highly-skewed long-tailed relation annotations,

i.e., the head predicate categories¹ have much more annotated ground-truth samples (or relation triplets) than the tail ones. Thus, a recent surge of interest in SGG is developing *unbiased* scene graph generation models, which can achieve more balanced performance on all predicate categories (*i.e.*, head, body, and tail categories). Currently, existing state-of-the-art unbiased SGG models can be coarsely grouped into four categories: 1) *Class-aware Re-sampling*: They try to sample more tail category training samples to balance the data distribution [18]. 2) *Loss Re-weighting*: They aim to reduce the contributions of the head categories training samples in the loss calculation by designing different weighting strategies [19], [20], [21]. 3) *Biased-model-based*: They disentangle unbiased representations from some biased trained models [22], [23], [24], [25]. 4) *Noisy Label Learning*: They first detect noisy annotated samples and then reassign them to more high-quality predicate labels [26], [27]. Although different advanced techniques have been proposed in each category, almost all existing unbiased SGG models follow the same training paradigm: *regarding the object and predicate classification as a single-label classification problem, and using the cross-entropy loss (between predicted distributions and one-hot target labels) as the training objective.*

Although today’s unbiased SGG models have achieved significant progress on some challenging SGG benchmarks (*e.g.*, VG), it is worth noting that this training paradigm has overlooked two characteristics of existing SGG datasets: 1) For the positive samples¹, some specific subject-object instances may have multiple reasonable predicates, *i.e.*, the semantics of different categories are not completely independent. For example in Fig. 1(a), predicates “on”, “sitting on”, “in”, and “above” are all reasonable predicates in these “man-chair” pairs. 2) For the negative samples, there are numerous missing annotations [28], and all these negative samples are treated as absolute background category in the training process. For instance, “boy-shirt”, “boy-helmet” in Fig. 1(b) are all missing-annotated subject-object instances. Similarly, some “negative” samples may even have multiple reasonable predicates (*e.g.*, “wearing” and “has” for “boy-shirt”).

By training the predicate classifier in SGG models with one-hot target labels, these neglected characteristics will respectively result in two adverse impacts: 1) It may lead to

*Long Chen is the corresponding author.

L. Li, H. Shi, W. Wang, J. Shao, Y. Yang and J. Xiao are with Zhejiang University, Hangzhou, 310027, China. Email: mukti@zju.edu.cn, hanrong@zju.edu.cn, wenxiaowang@zju.edu.cn, jshao@cs.zju.edu.cn, yangyics@zju.edu.cn, junx@cs.zju.edu.cn.

L. Chen is with Columbia University, New York, 10027, USA. Email: zjuchenlong@gmail.com.

¹For brevity, we directly use “tail”, “body”, and “head” categories to represent the predicate categories in the tail, body, and head parts of the number distributions of different ground-truth predicate annotations in SGG datasets, respectively. Besides, we use “positive” and “negative” samples to denote annotated ground-truth visual relation triplets with foreground and background predicate categories, respectively.

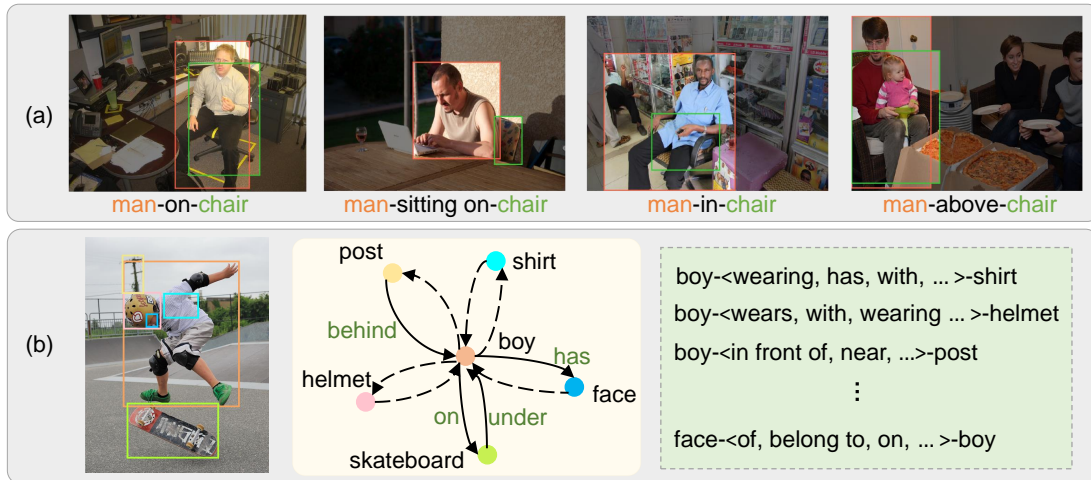


Fig. 1. Illustration of two overlooked characteristics in SGG benchmarks (take VG as an example). a) All listed `man-chair` pairs with similar visual appearance are assigned various predicates with semantic overlap and overlay. These predicates are also reasonable for other `man-chair` pairs. b) Images always have missing-annotated issues, and the missing-annotated triplets with one/many “reasonable” predicate(s) are directly treated as absolute `background`. Solid lines are annotated relations, dotted lines are missing-annotated, and green boxes are latent predicates for missing-annotated triplets.

confused SGG predictions by simply assigning one-hot target labels without considering multiple reasonable predicates for each subject-object pair. Meanwhile, some over-confident predictions on the head categories also enlarge the performance gap between different categories. 2) It may lead to wrong predictions by directly assigning absolute `background` (*i.e.*, one-hot target labels) to the missing-annotated subject-object pairs. Since the total probability is given to the wrong `background`, the model trusts the wrong label excessively.

To alleviate these issues, in this paper, we propose a novel model-agnostic Label Semantic Knowledge Distillation for unbiased SGG, dubbed **LS-KD**. Specifically, LS-KD integrates *label semantic distributions* (LSD, *i.e.*, the knowledge that reflects the correlations between subject-object instances and predicate categories) and original one-hot target labels to “soft” labels, and uses these “soft” labels to supervise the model training. Particularly, we utilize self-knowledge distillation (self-KD) to predict these LSDs, by transferring label semantic knowledge from a teacher model to the student model (*i.e.*, the model used for final prediction). Meanwhile, we propose two different self-KD strategies: 1) *Iterative self-KD*: the student model trained at an earlier step is utilized as the teacher model iteratively. 2) *Synchronous self-KD*: the student and teacher models share the same backbone with two different classifiers, and both models are trained synchronously. Thanks to these designs, the student model can utilize the past and current predictions (*i.e.*, LSD) of the teacher model in iterative and synchronous self-KD as informative supervision, respectively. Besides, we fuse the output of the teacher model with the original one-hot labels to generate soft target labels, which differs from other fusion strategies in the standard self-KD methods [29], [30], [31].

We evaluate our method on the most widely-used SGG benchmark: VG [12]. Since LS-KD is a model-agnostic debiasing method, it can be seamlessly incorporated into any advanced SGG architectures and consistently improve their performance. Extensive ablations and results on multiple SGG

tasks and backbones have shown the effectiveness and generalization ability of LS-KD.

In summary, we make three main contributions in this paper:

- 1) We are the first² to analyze the reason why the prevalent SGG training paradigm is unreasonable, *i.e.*, the effect of treating predicate classification in SGG as a single-label classification.
- 2) We propose a novel model-agnostic LS-KD, which can capture the correlations between the subject-object instances and different predicate categories.
- 3) We conduct extensive experiments to prove the superiority of LS-KD, which can achieve a decent trade-off performance between different predicates.

II. RELATED WORK

Scene Graph Generation (SGG). Scene graphs are structural representations that transform raw visual input into semantic categories. After Lu *et.al.* [28] firstly brought a large-scale dataset to attention, plentiful studies [32], [33] have been conducted in SGG. Existing SGG works can be divided into two groups: 1) Two-stage SGG: They first utilize a detector to obtain object proposals, then predict the classes of objects and their pairwise relations [34], [1], [35], [36], [37], [38], [39], [40], [41]. In order to exploit the rich global context, some works regard each image as a whole and adopt the fully connected graph [38], [39], the chained graph [37], and the tree-structured graph [40] to model the contexts among objects. 2) One-stage SGG: They use the fully convolutional network or Transformer to detect the objects and relations from image features directly [42], [43]. In this paper, we propose a model-agnostic debiasing method that can be used in any SGG model. In our experiments, two popular two-stage SGG models (Motifs [37] & VCTree [40]) are used as baselines.

²For “single-label classification”, we mean that *each triplet sample is assigned only one predicate label, and XE loss is used for training*. In contrast, all prior work only discussed that there may be more than one reasonable predicates for each subject-object pair.

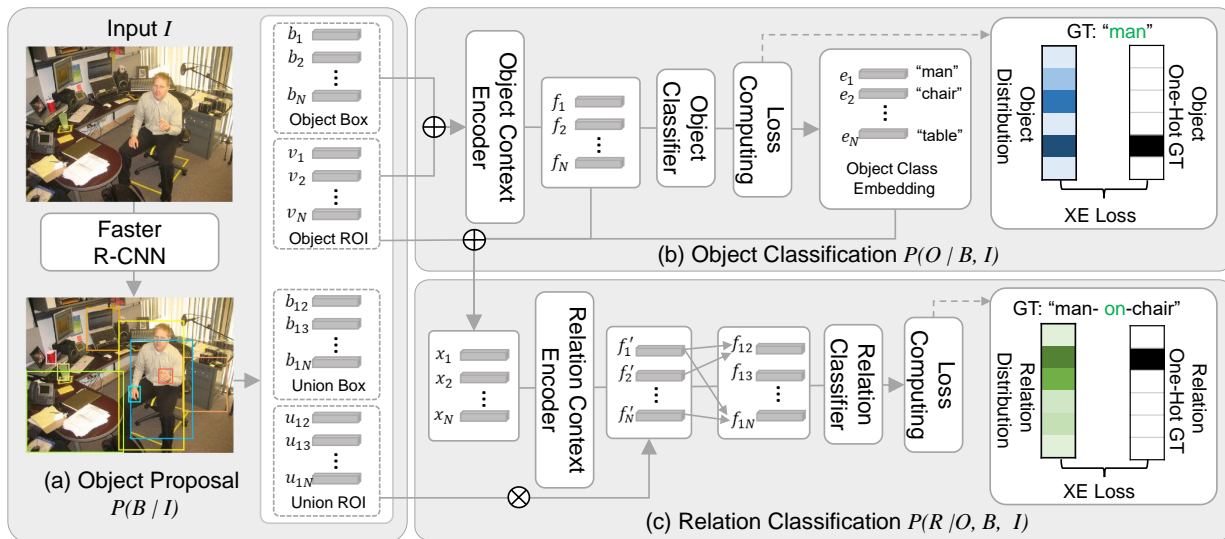


Fig. 2. The framework of SGG baseline. a) Object proposal module generates the bounding box proposals of objects. b) Object classification module predicts the class probabilities of object proposals. c) Relation classification module predicts the relation class probabilities of pairwise objects. \oplus denotes concatenation operation, \otimes denotes element-wise multiplication. Dotted line only shows one instance for loss calculation.

Unbiased Scene Graph Generation. Due to the long-tailed distribution and other language bias issues [44] in SGG, numerous recent SGG work mainly focuses on unbiased SGG [22], [15]. They can be roughly divided into four categories: 1) Class-aware Re-sampling: They balance the data distribution by oversampling samples of tail categories or undersampling of head ones, or a combination of both [18]. Specially, Desai *et al.* [45] resample both predicate and entity categories to balance the distribution of triplets. 2) Loss Re-weighting: They assign different weights to different categories to reduce the contributions of the head categories in loss calculation. These designed weights are often based on prior knowledge [19], [21] or learnable predicate correlations [20], and so on. 3) Biased-model-based: They try to separate unbiased predictions from biased trained models. For instance, Tang *et al.* [22] utilize counterfactual causality to separate biases from the biased model; Yu *et al.* [24] design a debiased reweight loss based on the biased model; Chiou *et al.* [23] recover the probability of unbiased prediction from the biased model. 4) Noisy Label Correction: They reformulate SGG as a noisy label learning problem and try to improve SGG annotation qualities. For example, Li *et al.* [26], [27] propose the NICE and NICEST strategy that can not only detect noisy samples but also reassign more high-quality predicate labels. In this paper, we try to capture the possibility between the instance and multiple relation labels, which achieves a trade-off between the head and tail categories.

Knowledge Distillation. Knowledge Distillation (KD) is a training strategy inspired by the “teacher-student” learning behavior, in which the teacher model is the exporter of knowledge and the student model is the receiver [46], [47], [48], [49], [50]. KD that can effectively learn a lightweight student model from a cumbersome teacher model has been widely used in numerous scene understanding applications, *e.g.*, VQA [51], scene graph generation [52]. Traditional KD

methods use knowledge from larger, better-performing teacher models to generate soft targets for student networks. Compared with conventional KD methods, self-knowledge distillation (self-KD) reduces the necessity of training a complicated teacher model in advance. It directly completes the distillation process with only the student network itself (*i.e.*, the teacher model and student model share the same network), and it has shown conspicuous performance [53], [54], [55], [56]. Since self-KD can capture the correlations between categories [57] and it does not require any additional networks, in this paper, we design two self-KD strategies (*i.e.*, iterative and synchronous) to predict the label semantic distribution.

Label Smoothing and Label Confusion. Label smoothing (LS) strategy [58], [59] is a regularization method, which has been widely used in classification tasks to prevent over-confident prediction and improve generalization ability. It typically combines a weighted uniform noise distribution with original one-hot target labels to obtain some softer labels for training. However, such soft labels generated merely by adding noise cannot reflect the correlations between each subject-object instance and multiple predicate categories. Label confusion (LC) method [60] is proposed in text classification task. It trains a label encoder to learn label representations and calculates the similarity between instances and labels to generate a better label distribution for training. Among these solutions, [60] is the closest to our approach, but we do not need to design additional network encoders to capture correlations between instances and multiple predicates. In addition, some semi-supervised SGG methods also assign soft labels to unannotated samples [61], [62].

III. APPROACH

Scene Graph Definition. Given an image I , a scene graph is formally represented by $\mathcal{G} = \{ \mathcal{N} = \{ o_i; b_i \}; \mathcal{E} = \{ r_{ij} \} \}$, where the \mathcal{N} and \mathcal{E} denote the set of nodes and the set of

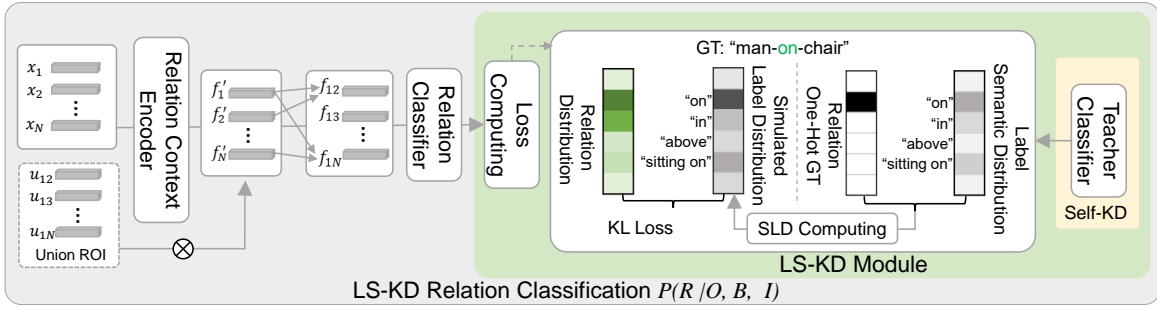


Fig. 3. Overview of the LS-KD relation classification, which adds an LS-KD module to the baseline relation classification module. The green box represents the LS-KD module. The dotted line indicates an instance case when calculating loss.

edges, respectively. $o_i \in O$ denotes the object category of the i -th object, and its bounding box is $b_i \in B$. $r_{ij} \in R$ denotes the relation category between i -th object and j -th object. B , O , and R represent the set of all predicted bounding boxes, object categories, and relation categories, respectively.

In this section, we first revisit the general SGG baseline in Section III-A, then present details of the proposed Label Semantic Knowledge Distillation (LS-KD) in Section III-B, and details of two self-KD strategies in Section III-C.

A. Revisit Scene Graph Generation Baselines

As shown in Fig. 2, the most common SGG framework typically consists of three modules: object proposal, object classification and relation classification. These frameworks decompose the SGG target $P(\mathcal{G}|I)$ into three steps:

$$P(\mathcal{G}|I) = P(B|I)P(O|B, I)P(R|O, B, I), \quad (1)$$

where $P(B|I)$ is predicted by the object proposal module, $P(O|B, I)$ is predicted by the object classification module, and $P(R|B, O, I)$ is predicted by the relation classification module. In the following, we briefly introduce these modules.

1) *Object Proposal Module*.: This module is to model $P(B|I)$. Given an image I , bounding box b_i of each proposal is obtained by using a standard object detector (e.g., Faster R-CNN [13]). Visual feature v_i corresponding to each proposal region is extracted with RoIAlign operation [63]. Similarly, we compute the union box b_{ij} of the i -th and j -th detected object region and extract the union visual features u_{ij} in the same way. The union region provides contextual information about the interactions between objects to aid relation classification.

2) *Object Classification Module*.: It is composed of an object context encoder and an object classifier to model $P(O|B, I)$. The object context encoder $\text{Encoder}_{\text{obj}}$ takes the object ROI features $\{v_i\}$ and bounding boxes $\{b_i\}$ as input and outputs the object context representation $\{f_i\}$:

$$f_i = \text{Encoder}_{\text{obj}}(v_i \oplus b_i), \quad (2)$$

where \oplus denotes concatenation operation. Some SGG work adopts bi-directional LSTMs [37], bi-directional TreeLSTMs [40] or fully connected layers [64], [65] to encode context information among objects. The object classifier utilizes the fully-connected layer FC followed by a softmax operation

with temperature τ to model $P(B|O, I)$ and predict object classes $\{o_i\}$:

$$\text{FC}(W, \sigma, f) = W^T f + \sigma, \quad (3)$$

$$\hat{y}_i^o = \text{Softmax}(\text{FC}(W_o, f_i, \sigma_o), \tau), \quad (4)$$

where W and σ are learnable weight and bias of the fully-connected layer, \hat{y}_i^o is the predicted label distribution of the object o_i .

3) *Relation Classification Module*.: It consists of two parts: a relation context encoder and a relation classifier to model $P(R|O, B, I)$. The relation context encoder $\text{Encoder}_{\text{rel}}$ takes the joint feature embeddings $\{x_i\}$ as input and outputs the refined object features $\{f'_i\}$:

$$x_i = v_i \oplus f_i \oplus e_i, \quad (5)$$

$$f'_i = \text{Encoder}_{\text{rel}}(x_i), \quad (6)$$

where e_i is the word embedding of object class o_i . The pairwise refined object features mixed with union feature u_{ij} to obtain the relation representation f_{ij} between the i -th and j -th objects. The relation classifier is similar to object classifier but with different categories to predict the label distribution:

$$f_{ij} = [f'_i \oplus f'_j] \otimes u_{ij}, \quad (7)$$

$$\hat{y}_{ij}^r = \text{Softmax}(\text{FC}(W_r, f_{ij}, \sigma_r), \tau), \quad (8)$$

where \otimes denotes element-wise multiplication, \hat{y}_{ij}^r is the predicted label distribution of predicate r_{ij} . W_r and σ_r are parameters of FC for relation classification.

4) *Training Strategy*.: The object proposal module is frozen during training, while the two classification modules are trained using standard cross-entropy (XE) loss \mathcal{L}_o and \mathcal{L}_r with one-hot object and relation target labels, respectively, i.e.,

$$\mathcal{L}_o = \text{XE}(y^o, \hat{y}^o) = -y^o \log(\hat{y}^o), \quad (9)$$

$$\mathcal{L}_r = \text{XE}(y^r, \hat{y}^r) = -y^r \log(\hat{y}^r), \quad (10)$$

where y^o and y^r denotes the object and relation one-hot target labels respectively, \hat{y}^o and \hat{y}^r is the predicted object and relation label distribution.

B. LS-KD Relation Classification

To alleviate the issues mentioned in Section I caused by the training relation classifier just with one-hot target labels, we design an LS-KD relation classification with soft labels

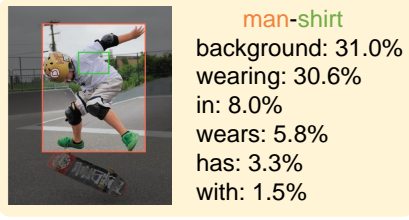


Fig. 4. An example of the LSD of a missing-annotated triplet.

that consider the correlations between instances and multiple predicate categories. Taking triplet “man-on-chair” in Fig. 3 as an example, LS-KD can assign a portion of probability to predicate labels related to the “man-chair”, such as “sitting on”, “in” and “above” rather than give full probability to the one-hot label “on”. Compared to the basic relation classification, the LS-KD relation classification adds an extra LS-KD module.

The label semantic knowledge distillation module is constructed by an output of the teacher model classifier trained by self-KD and a simulated label distribution computing block. The details of self-KD learning will be described in Section III-C. The teacher model classifier takes the relation representations $\{f_{ij}\}$ extracted by the relation encoder as an input and outputs Label Semantic Distributions (LSDs). The LSD can dynamically capture the correlations among multiple predicate categories for each instance. Finally, we adopt a controlling hyperparameter α to merge the original one-hot vector and LSD and then utilize a softmax function to generate the final Simulated Label Distribution (SLD). The SLD is used as the soft target label to replace the one-hot vector to supervise the training of the relation classifier. The hyperparameter α determines the proportion of the final fusion between the LSDs and the original one-hot target labels:

$$y_{ij}^t = \text{Softmax}(\text{FC}(W, f_{ij}, \sigma), \tau), \quad (11)$$

$$y_{ij}^s = \text{Softmax}(\alpha y_{ij}^r + y_{ij}^t, \tau), \quad (12)$$

where y_{ij}^t is the output LSD of the teacher model classifier, y_{ij}^r is the original one-hot vector of the predicate label, and y_{ij}^s is the computed SLD. With the early supervision of the original single label, the output of the teacher model can reflect the correlations between each subject-object pair and multiple predicate categories. However, the probability gap between head and tail categories is large due to the long-tail distribution, which results in excessive suppression of reasonable tail predicates. Thus, we let the model learn more reasonable y_{ij}^t that can soften the original labels to reduce the gap between head and tail predicates. Meanwhile, the supervision in our method is the pseudo label distribution y_{ij}^s .

During training, we adopt KL-divergence [66] loss to measure the similarity between two probability distributions (the SLD y_{ij}^s and the predicted relation label distribution \widehat{y}_{ij}^r):

$$\mathcal{L}_r = \text{KL}(y^s, \widehat{y}^r) = \sum_c y_c^s \log\left(\frac{y_c^s}{\widehat{y}_c^r}\right), \quad (13)$$

where $c \in C$ represents c -th predicate category. Through the training of the LS-KD module, the soft target dynamically changes for each triplet instance based on the semantic knowledge learned by the teacher model among predicate labels.

The learned simulated label distribution not only contributes to better representing the instance with multiple confusing predicate labels, but also it is more robust to missing-annotated triplets. For the missing-annotated subject-predicate-object triplets, a portion of the probability of the original one-hot background label is allocated to some reasonable foreground predicate labels (e.g., “wearing”, “in”, and other predicates for the “man-chair” pair in Fig. 4), thus the model can still learn some label semantic knowledge.

C. Self-Knowledge Distillation for LSD

Since the probabilistic output of the teacher model in self-KD can reflect the correlations of multiple predicate labels for each instance, it does not require the design of an extra model structure (i.e., the student and teacher models share the same network). In this paper, we explore two different self-KD strategies: iterative self-KD and synchronous self-KD, to prompt the teacher model to predict label semantic distributions. The pipelines are shown in Fig. 5.

1) *Iterative Self-Knowledge Distillation.*: During the training, the student model becomes the teacher model itself iteratively. By iterative self-KD, the student model can utilize its past predictions to serve more informative supervisions (i.e., label semantic knowledge) for training. Concretely, the student model of the $(t-1)$ -th epoch becomes the teacher model during training in (t) -th epoch, and the parameters of the teacher model are frozen. The outputs of the teacher model are fused with one-hot target labels by hyperparameter α in the LS-KD module to generate soft labels. These soft labels are utilized to supervise the student model training with KL loss. Especially when training at the first epoch, we just utilize a cross-entropy loss with the one-hot label to train the student model.

2) *Synchronous Self-Knowledge Distillation.*: During the training, the student model and the teacher model share the same relation encoder. However, they adopt two pseudo-siamese classifier heads (i.e., the networks with the same structure but different parameters): the teacher distill head and the student classifier head. These two heads take the same relation representations $\{f_{ij}\}$ as input. The difference is that the teacher distill head is trained by cross-entropy loss with one-hot labels. Similarly, the output of the teacher distill head is used in the LS-KD to generate soft target labels to supervise the training of the student classifier head by KL loss.

Comparison with Prior Self-KD Models. Our fusion strategy of the original one-hot label and the output of teacher model differs from all the standard self-KD methods [29], [30], [31]. More importantly, our motivation and main contributions are to model the correlation between multiple predicates for each sub-obj instance. To achieve the goal, we resorted to KD to generate soft labels for supervised training. In addition, to avoid designing additional model structures, we adopted self-KD strategy and proposed two variants.

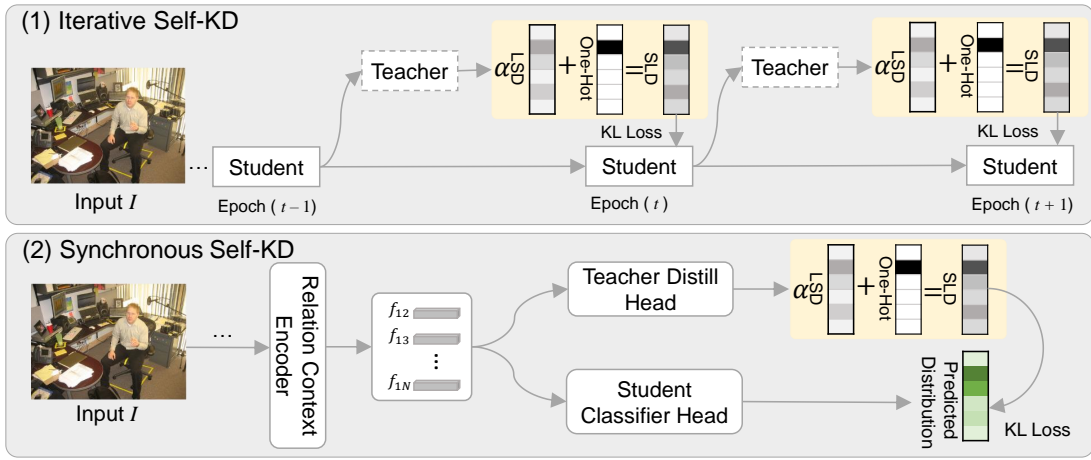


Fig. 5. The pipeline of two self-Knowledge Distillation learning strategies. When training in t epoch, student model trained at $t - 1$ epoch becomes the teacher model. Dotted lines indicate that the model weights are frozen.

IV. EXPERIMENTS

A. Experimental Settings and Details

Datasets. We conducted the experiments on the most prevalent SGG benchmark: Visual Genome (VG) [12] that totally contains 108,073 images. Since the number of samples in most predicate categories is quite limited, in our experiments, we followed the widely-used data splits [1], which consists of 150 object categories and 50 predicate categories. The dataset is split with 70% of images as the training set and the other 30% as the testing set, respectively. Following the same protocol in [37], We sampled 5000 images from the training set as the validation set for hyperparameter tuning.

Tasks. We evaluated the model on the three SGG tasks [1]: 1) *Predicate Classification (PredCls)*: Given the ground-truth object bounding boxes with ground-truth object classes, the model is required to predict the predicate categories of object pairs. 2) *Scene Graph Classification (SGCls)*: Given the ground-truth object bounding boxes without classes, the model is required to predict both the object categories and predicate categories. 3) *Scene Graph Generation (SGGen)*: Given an image, the model is required to detect all object bounding boxes, and predict categories of both the object and predicate.

Metrics. We evaluated all results on three metrics: 1) *Recall@K (R@K)*: It calculates the fraction of the top K confident predicted subject-relation-object triplets that match the ground-truth. In this paper, we utilized $K = \{50, 100\}$. 2) *mean Recall@K (mR@K)*: It retrieves each predicate separately and then averages the R@K for all predicates, we also reported $K = \{50, 100\}$. 3) **Mean**: It is the average of all mR@K and R@K scores. Since R@K favors head predicates and mR@K favors tail predicates, the Mean metric is better for evaluating the performance across all predicates. For unbiased SGG, mR@K is often boosted at the cost of the drop in R@K (*i.e.*, many state-of-the-art debiasing models [23], [22], [24] suffer from obvious performance drops on head predicates), and thus Mean is a comprehensive metric to measure the performance on different predicate categories [26].

Implementation Details. Following the similar protocol in [22], we adopted Faster R-CNN with the ResNeXt-101-FPN [67] backbone to detect object bounding boxes and extract RoI features, and kept the parameters frozen during the training. We utilized the detector trained by [22], which achieved 28.14 mAP on the VG test set (*i.e.*, using 0.5 IoU threshold). The hyperparameter α utilized in LS-KD relation classification was set to 4, and temperature τ of two self-KD were set to 1. The confidence of a predicted triplet is calculated by multiplying the classification score of three components (*i.e.*, subject, object and predicate). The models in this paper were trained by SGD optimizer, where the mini-batch size was 12, and the initial learning rate was 0.01. After the validation performance plateaus, the learning rate would be decayed by 10 two times. All the experiments were implemented with PyTorch and conducted with NVIDIA 2080ti GPUs.

B. Comparison with State-of-the-Arts

Settings. We conducted LS-KD with iterative and synchronous self-KD on the two popular baselines (Motifs [37] and VCTree [40]), denoted as **LS-KD (Iter)** and **LS-KD (Syn)** respectively. In Table I, we listed the results of the various state-of-the-art SGG models for reference, and divided them into two groups: 1) The methods are not model-agnostic debiasing models, including MSDN [68], G-RCNN [38], and DT2ACBS [45]. 2) The methods are model-agnostic debiasing strategies, including TDE [22], PCPL [20], CogTree [24], DLFE [23], and BP-LSA [25]. Since LS-KD is model-agnostic, we mainly compared with methods in the second group with the same baselines. To further illustrate the performance of our model, we show recall statistics for each predicate of LS-KD, TDE [22], and Motifs [37] in Fig. 6 for comparisons. Besides, we report the R@100 metric of each predicate category group under the PredCls setting in Table II. **Results.** From the results in Table I, we find that: 1) LS-KD exceeds the performance of baseline models under all the three settings and achieves comparable performance with some SOTA methods (*e.g.*, TDE, PCPL and DLFE) in the mR@K metrics. 2) LS-KD achieves a better trade-off between the

TABLE I
PERFORMANCE (%) OF STATE-OF-THE-ART SGG MODELS ON THREE SGG TASKS. “MEAN” IS THE AVERAGE OF MR@50/100 AND R@50/100.

Models	PredCls			SGCls			SGGen		
	mR@50/100	R@50/100	Mean	mR@50/100	R@50/100	Mean	mR@50/100	R@50/100	Mean
MSDN [68]	15.9/17.5	64.6/66.6	41.2	9.3/9.7	38.4/39.8	24.3	6.1/7.2	31.9/36.6	20.5
G-RCNN [38]	16.4/17.2	64.8/66.7	41.3	9.0/9.5	38.5/37.0	23.5	5.8/6.6	29.7/32.8	18.7
DT2ACBS [45]	35.9/39.7	23.3/25.6	31.1	24.8/27.5	16.2/17.6	21.5	22.0/24.4	15.0/16.3	19.4
Motifs+TDE [22]	24.2/27.9	45.0/50.6	36.9	13.1/14.9	27.1/29.5	21.2	9.2/11.1	17.3/20.8	14.6
Motifs+PCPL [20]	24.3/26.1	54.7/56.5	40.4	12.0/12.7	35.3/36.1	24.0	10.7/12.6	27.8/31.7	20.7
Motifs+CogTree [24]	26.4/29.0	35.6/36.8	32.0	14.9/16.1	21.6/22.2	18.7	10.4/11.8	20.0/22.1	16.1
Motifs+DLFE [23]	26.9/28.8	52.5/54.2	40.6	15.2/15.9	32.3/33.1	24.1	11.7/13.8	25.4/29.4	20.1
Motifs+BPL-SA [25]	29.7/31.7	50.7/52.5	41.2	16.5/17.5	30.1/31.0	23.8	13.5/15.6	23.0/26.9	19.8
Motifs+LS-KD(Iter)	24.1/27.4	55.1/59.1	41.4	13.8/15.2	33.8/35.8	24.7	9.7/11.5	25.6/29.7	19.1
Motifs+LS-KD(Syn)	22.3/25.3	56.9/60.3	41.2	12.4/14.1	35.4/37.1	24.8	8.1/10.0	27.5/31.6	19.3
VCTree+TDE [22]	26.2/29.6	44.8/49.2	37.5	15.2/17.5	28.8/32.0	23.4	9.5/11.4	17.3/20.9	14.8
VCTree+PCPL [20]	22.8/24.5	56.9/58.7	40.7	15.2/16.1	40.6/41.7	28.4	10.8/12.6	26.6/30.3	20.1
VCTree+CogTree [24]	27.6/29.7	44.0/45.4	36.7	18.8/19.9	30.9/31.7	25.3	10.4/12.1	18.2/20.4	15.3
VCTree+DLFE [23]	25.3/27.1	51.8/53.5	39.4	18.9/20.0	33.5/34.6	26.8	11.8/13.8	22.7/26.3	18.7
VCTree+BPL-SA [25]	30.6/32.6	50.0/51.8	41.3	20.1/21.2	34.0/35.0	27.6	13.5/15.7	21.7/25.5	19.1
VCTree+LS-KD(Iter)	24.2/27.1	55.7/59.5	41.6	17.3/19.1	38.4/40.5	28.8	9.7/11.3	25.3/29.5	19.0
VCTree+LS-KD(Syn)	22.0/25.4	57.5/60.8	41.4	14.6/16.5	40.6/42.6	28.6	8.2/10.1	27.5/31.2	19.3

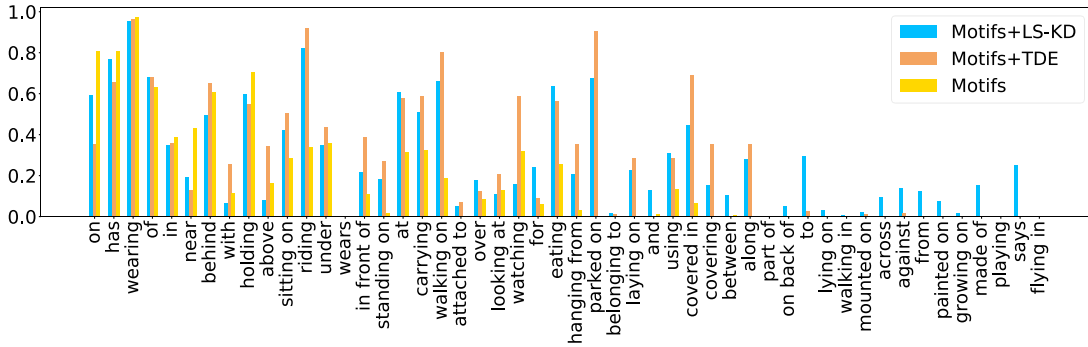


Fig. 6. Recall statistics for each predicate category. The baseline model is Motifs [37].

TABLE II
RECALL@100 OF EACH GROUP, *i.e.*, HEAD, BODY AND TAIL, UNDER PREDCLS SETTING. MEAN IS THE AVERAGE OF THREE GROUPS.

Models	PredCls R@100			
	Head	Body	Tail	MEAN
Motifs [37]	80.5	29.3	5.7	42.3
+TDE [22]	66.4	40.1	20.3	38.5
+LS-KD	74.9	35.5	20.5	43.6

TABLE III
COMPARISON WITH LS AND LC. THE BASELINE MODEL IS MOTIFS [37].

Methods	PredCls		
	mR@50/100	R@50/100	Mean
Motifs+Label Smooth (LS)	24.6 / 27.9	50.6 / 55.8	39.7
Motifs+Label Confusion (LC)	25.1 / 28.6	50.3 / 55.3	39.8
Motifs+LS-KD	24.1 / 27.4	55.1 / 59.1	41.4

R@K and mR@K, and surpasses the state-of-the-art method in the Mean metric under both PredCls and SGCls settings (*e.g.*, 41.2% in BPL-SA vs. 41.4% in LS-KD, 23.8 % in BPL-SA vs. 24.8% in LS-KD based on Motifs). To the best of our knowledge, all SOTA debiasing SGG models have lower performance than the baseline for the Mean metric. In contrast, our LS-KD has the least performance drops on the head predicates (*cf.* R@K) and keeps the performance of tail predicates (*cf.* mR@K), which proves the superiority of LS-KD by synthesizing all predicates. 3) LS-KD (Syn) can achieve higher performance than LS-KD (Iter) on R@K, because the teacher head of LS-KD (Syn) is trained by cross-entropy loss with one-hot target labels, which is susceptible to the influence of long-tailed distributions. Furthermore, as shown in Fig. 6 and Table II, we can observe that our proposed LS-KD could achieve a decent trade-off among different predicate categories (*e.g.*, 38.5% in TDE vs. 43.6% in LS-KD

in the Mean metric under PredCls settings based on Motifs).

C. Comparison with Label Smoothing and Confusion

Settings. In Table III, we re-implemented the general Label Smoothing (LS) [69] and Label Confusion (LC) [60] methods under the PredCls setting for SGG. LS softens one-hot targets by adding uniform distribution. LC captures semantic overlap among labels by calculating the similarity between instances and labels, and generates soft targets for training. For a fair comparison, all the α controlling the synthesis of the original one-hot vector and soft distribution were set to 4.

Results. From the results, we get the following findings: 1) By making the model less confident during training, the LS method can alleviate the over-fitting of the model to a certain extent, especially for the head predicate classes that account for a large proportion. LS only softens the targets by adding uniformly distributed noise. Thus, it cannot reflect the correlations among predicates labels, resulting in poor performance

TABLE IV
ABLATION STUDIES ON THE HYPERPARAMETER α OF LS-KD WITH ITERATIVE SELF-KD AND SYNCHRONOUS SELF-KD. THE BASELINE MODEL IS MOTIFS [37].

α	Type	PredCls		
		mR@50/100	R@50/100	Mean
-	-	16.5 / 17.8	65.5 / 67.2	41.8
3	Iter	25.6 / 29.6	43.5 / 49.8	37.1
	Syn	24.2 / 28.3	44.9 / 51.0	37.1
4	Iter	24.1 / 27.4	55.1 / 59.1	41.4
	Syn	22.3 / 25.3	56.9 / 60.3	41.2
5	Iter	20.6 / 23.0	60.7 / 63.5	42.0
	Syn	18.8 / 21.0	61.7 / 64.1	41.4

on Mean (39.7% in LS vs. 41.4% in LS-KD). 2) The LC method can achieve better results on mR@K, but it is inferior to our method in the performance on Mean (39.8% in LC vs. 41.4% in LS-KD) that considers all predicates synthetically. Besides, it needs to design additional networks to encode the representation of labels, and it takes a lot of time to calculate the similarity among all labels for each instance. 3) Both LS and LC methods can significantly improve the performance in the mR@K compared with the baseline performance, which means LS and LC are helpful even without using a teacher-student model. However, since our motivation is to generate soft labels that can reflect the correlations between subject-object pairs and multiple predicates, we adopt KD whose output is a probability distribution. Meanwhile, as the training target is soft labels, it cannot depart from multi-label paradigm.

D. Ablation Studies

1) *Ablation Study on α in LS-KD.*: In Table IV, we set various hyperparameters α in LS-KD to control the degree of fusion between the LSD learned by the teacher model and the original one-hot vector. The larger α , the larger weight will be assigned to the one-hot vector when generating a soft label in the SLD module.

When the hyperparameter α is set to 5, the original one-hot vector takes a larger proportion than the other two values (*i.e.*, 3 and 4), and the model makes over-confident predictions on head predicate with larger sample size, so the R@K is relatively high. When the hyperparameter α is set to 3, the LSD accounts for a greater proportion than the other two values (*i.e.*, 4 and 5). If the instance is related to multiple labels, the sample will not excessively fit just one label, and the probability gap between head and tail predicate categories will decrease relatively. Therefore, mR@K is relatively high.

Also, since α is a hyperparameter for the trade-off between Recall and Mean Recall performance, we plot the mR-R curve of all the operating results in Fig. 7. As shown in Fig. 7, almost all prior debiasing methods are under this curve, which confirms the effectiveness of our proposed method.

2) *Ablation Study on the Temperature τ in LS-KD.*: In Table V, we set the different temperature τ of softmax function in LS-KD. The larger τ is, the smoother the output probability distribution of softmax is. From the results, we find that the smoother the LSD, the better the performance on mR@K, and the steeper the LSD, the better the performance on R@K.

TABLE V
ABLATION STUDIES ON THE TEMPERATURE τ OF LS-KD WITH ITERATIVE SELF-KD AND SYNCHRONOUS SELF-KD. THE BASELINE MODEL IS MOTIFS [37].

τ	Type	PredCls		
		mR@50/100	R@50/100	Mean
-	-	16.5 / 17.8	65.5 / 67.2	41.8
0.1	Iter	23.6 / 26.7	55.7 / 59.7	41.4
	Syn	21.1 / 24.1	57.1 / 60.6	40.7
1	Iter	24.1 / 27.4	55.1 / 59.1	41.4
	Syn	22.3 / 25.3	56.9 / 60.3	41.2
10	Iter	24.2 / 28.0	51.7 / 57.3	40.3
	Syn	22.3 / 26.0	51.9 / 56.9	39.3

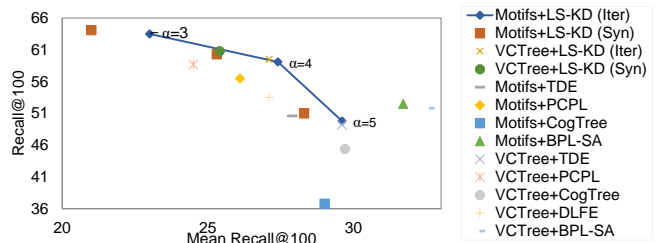


Fig. 7. The mR-R curve of SOTA models under PredCls setting.

TABLE VI
ABLATION STUDIES ON THE ITERATIVE INTERVAL t OF ITERATIVE SELF-KD. THE BASELINE MODEL IS MOTIFS [37]. 0.5 ITERATION MEANS THE ITERATION PERIOD IS 0.5 EPOCH.

t	PredCls		
	mR@50/100	R@50/100	Mean
-	16.5 / 17.8	65.5 / 67.2	41.8
0.5	24.0 / 27.3	54.6 / 58.9	41.2
1	24.0 / 27.2	54.8 / 59.2	41.3
2	24.1 / 27.4	55.1 / 59.1	41.4

3) *Ablation Study on Iterative Interval t of Iterative Self-KD.*: We conducted experiments with different iterative intervals t of iterative self-KD (*i.e.*, the interval of iterations to transform the student model into the teacher model). Observing the results, we can find that the larger the iteration interval, the higher the performance on Mean.

E. Qualitative Results

1) *Generated Scene Graphs.*: Some generated scene graphs are visualized in Fig. 8, where the scene graphs with a yellow background are generated by Motifs-baseline, and those with a green background are by Motifs-Ours. Only the top-1 prediction and detected boxes overlapped with GT are shown. Comparing the results of the two methods, we can find that our method can detect more informative predicates, such as “laying on”, “sitting on”, and “carrying”. These predicates all have corresponding head predicates that have overlapping or overlaying semantics with them, such as “on” and “with”. The reason may be that we can reduce the margin of possibility between the head and tail predicates with similar semantics by capturing the correlation of the instance to multiple predicates. Thus, the over-confident predictions on head predicates under long-tailed distribution can be alleviated to some extent. Besides, for triplets that are hard

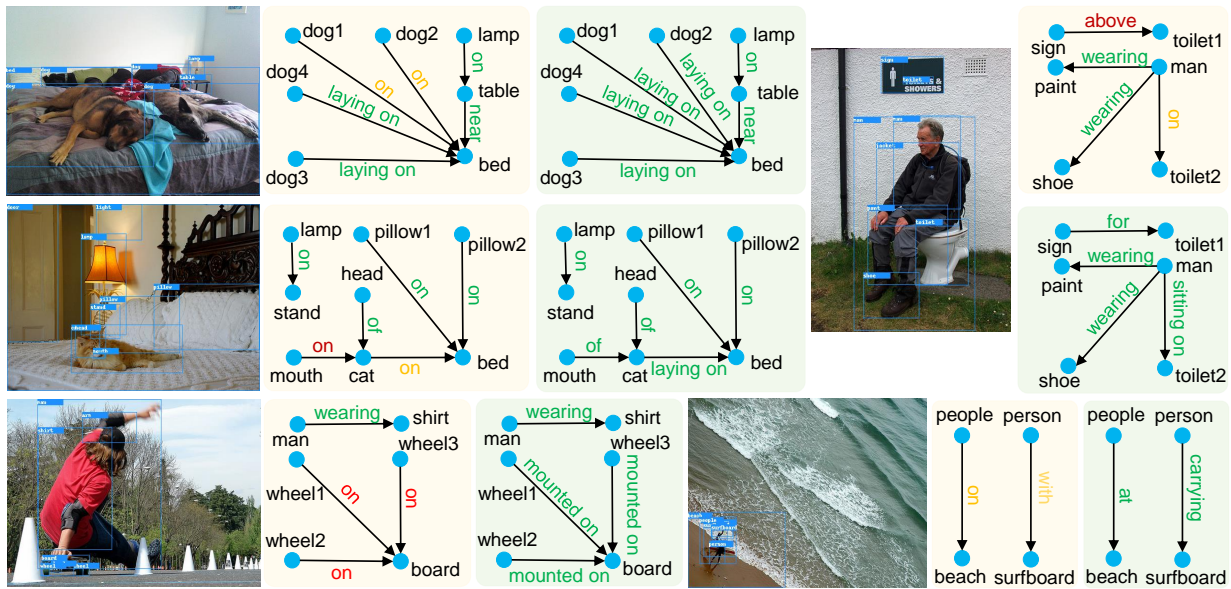


Fig. 8. Results of scene graphs generated from Motifs-baseline (yellow) and Motifs-Ours (green) in PredCls. Green predicates are correct (i.e., match GT), yellow predicates are acceptable (i.e., does not match GT but still reasonable), and red predicates are incorrect (i.e., does not match GT and unreasonable).

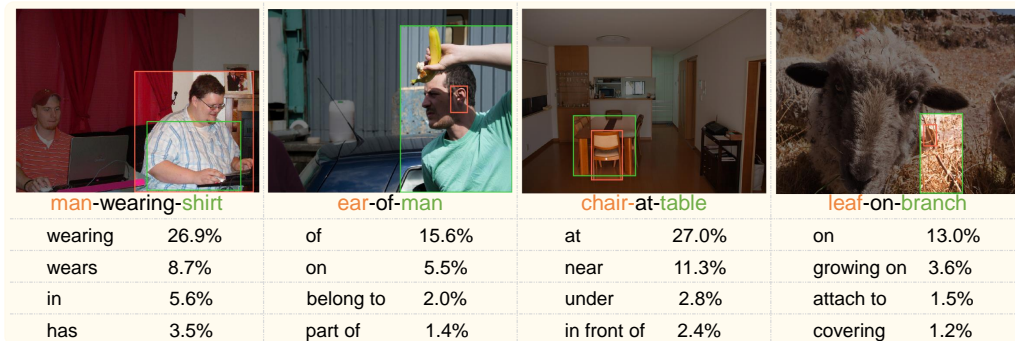


Fig. 9. Results of top 4 predicate categories that are most relevant to the triplet instance without background category.

to predict (e.g., “wheel-mounted on-board” and “sign-for-toilet”), Motifs-baselines are susceptible to frequency bias to make incorrect predictions (e.g., “wheel-on-board” and “sign-above-toilet”), while the predictions of our method are correct. It confirms that reducing the overfitting to the head predicates by training with soft labels is effective.

2) *Label Semantic Knowledge Distillation Module.*: In Fig. 9, we displayed the top 4 predicate categories derived from the iterative self-KD in label semantic knowledge distillation module that are most relevant to each subject-predicate-object triplet instance. From the results, we can observe that these predicate categories associated with a specific instance are all reasonable and even more valuable and informative to the subject-object pair. For example, for the “chair-at-table” triplet, the two predicate categories “under” and “in front of” capture the spatial position relationship between the “chair” and the “table” from different angles, and these more exact predicates are more valuable than “at”. In addition, for the “leaf-on-branch” triplet, predicates “growing on” and “covering” represent a dynamic relationship that is more informative than the static “on”. Besides, the predicate category with the max

proportion is still GT (i.e., best answer), and the other reasonable tail predicates (i.e., a fair but generally good answer) are assigned proportional probabilities. Thus, the soft labels generated by LS-KD can avoid the over-fitting of the head predicates and promote unbiased prediction to a certain extent.

V. CONCLUSIONS AND FUTURE WORK

In this paper, we point out the drawbacks of the prevalent training paradigm in existing SGG works, i.e., training the predicate classifier with one-hot target labels. To alleviate these drawbacks, we present a novel model-agnostic LS-KD for unbiased SGG. Two different self-KD strategies are designed in LS-KD to predict label semantic distribution (LSD): iterative self-KD and synchronous self-KD. LSD can not only reflect the correlations between subject-object instances and multiple predicate categories, but also generate more robust “soft” pseudo labels. Extensive results have proved the generality and effectiveness of our method. Moving forward, we are going to: 1) integrate LS-KD into existing debiasing methods whose goal is to solve the long-tailed distribution problem. 2) design better methods to capture correlations among predicate labels.

ACKNOWLEDGMENTS

This work was supported by the National Key Research & Development Project of China (2021ZD0110700), the National Natural Science Foundation of China (U19B2043, 61976185), Zhejiang Natural Science Foundation (LR19F020002), Zhejiang Innovation Foundation(2019R52002), and the Fundamental Research Funds for the Central Universities.

REFERENCES

- [1] D. Xu, Y. Zhu, C. B. Choy, and L. Fei-Fei, "Scene graph generation by iterative message passing," in *Proceedings of the IEEE conference on computer vision and pattern recognition*, 2017, pp. 5410–5419.
- [2] X. Yang, K. Tang, H. Zhang, and J. Cai, "Auto-encoding scene graphs for image captioning," in *Proceedings of the IEEE/CVF Conference on Computer Vision and Pattern Recognition*, 2019, pp. 10 685–10 694.
- [3] X. Li and S. Jiang, "Know more say less: Image captioning based on scene graphs," *IEEE Transactions on Multimedia*, vol. 21, no. 8, pp. 2117–2130, 2019.
- [4] J. Gu, S. Joty, J. Cai, H. Zhao, X. Yang, and G. Wang, "Unpaired image captioning via scene graph alignments," in *Proceedings of the IEEE/CVF International Conference on Computer Vision*, 2019, pp. 10 323–10 332.
- [5] L. Yu, J. Zhang, and Q. Wu, "Dual attention on pyramid feature maps for image captioning," *IEEE Transactions on Multimedia*, vol. 24, pp. 1775–1786, 2021.
- [6] Y. Mao, L. Chen, Z. Jiang, D. Zhang, Z. Zhang, J. Shao, and J. Xiao, "Rethinking the reference-based distinctive image captioning," in *ACM International Conference on Multimedia*, 2022.
- [7] J. Johnson, R. Krishna, M. Stark, L.-J. Li, D. Shamma, M. Bernstein, and L. Fei-Fei, "Image retrieval using scene graphs," in *Proceedings of the IEEE/CVF Conference on Computer Vision and Pattern Recognition*, 2015, pp. 3668–3678.
- [8] C. Bai, H. Li, J. Zhang, L. Huang, and L. Zhang, "Unsupervised adversarial instance-level image retrieval," *IEEE Transactions on Multimedia*, vol. 23, pp. 2199–2207, 2021.
- [9] J. Shi, H. Zhang, and J. Li, "Explainable and explicit visual reasoning over scene graphs," in *Proceedings of the IEEE/CVF Conference on Computer Vision and Pattern Recognition*, 2019, pp. 8376–8384.
- [10] W. Zhang, S. Tang, Y. Cao, S. Pu, F. Wu, and Y. Zhuang, "Frame augmented alternating attention network for video question answering," *IEEE Transactions on Multimedia*, vol. 22, no. 4, pp. 1032–1041, 2019.
- [11] L. Chen, X. Yan, J. Xiao, H. Zhang, S. Pu, and Y. Zhuang, "Counterfactual samples synthesizing for robust visual question answering," in *Proceedings of the IEEE/CVF Conference on Computer Vision and Pattern Recognition*, 2020, pp. 10 800–10 809.
- [12] R. Krishna, Y. Zhu, O. Groth, J. Johnson, K. Hata, J. Kravitz, S. Chen, Y. Kalantidis, L.-J. Li, D. A. Shamma *et al.*, "Visual genome: Connecting language and vision using crowdsourced dense image annotations," *International journal of computer vision*, vol. 123, no. 1, pp. 32–73, 2017.
- [13] S. Ren, K. He, R. Girshick, and J. Sun, "Faster r-cnn: Towards real-time object detection with region proposal networks," *Advances in neural information processing systems*, vol. 28, 2015.
- [14] W. Li, H. Zhang, Q. Bai, G. Zhao, N. Jiang, and X. Yuan, "Ppdl: Predicate probability distribution based loss for unbiased scene graph generation," in *Proceedings of the IEEE/CVF Conference on Computer Vision and Pattern Recognition (CVPR)*, 2022, pp. 19 447–19 456.
- [15] X. Han, X. Song, X. Dong, Y. Wei, M. Liu, and L. Nie, "Dbiased-p: Dual-biased predicate predictor for unbiased scene graph generation," *IEEE Transactions on Multimedia*, pp. 1–11, 2022.
- [16] X. Dong, T. Gan, X. Song, J. Wu, Y. Cheng, and L. Nie, "Stacked hybrid-attention and group collaborative learning for unbiased scene graph generation," in *Proceedings of the IEEE/CVF Conference on Computer Vision and Pattern Recognition (CVPR)*, 2022, pp. 19 427–19 436.
- [17] A. Goel, B. Fernando, F. Keller, and H. Bilen, "Not all relations are equal: Mining informative labels for scene graph generation," in *Proceedings of the IEEE/CVF Conference on Computer Vision and Pattern Recognition (CVPR)*, 2022, pp. 15 596–15 606.
- [18] R. Li, S. Zhang, B. Wan, and X. He, "Bipartite graph network with adaptive message passing for unbiased scene graph generation," in *Proceedings of the IEEE/CVF Conference on Computer Vision and Pattern Recognition*, 2021, pp. 11 109–11 119.
- [19] T.-Y. Lin, P. Goyal, R. Girshick, K. He, and P. Dollár, "Focal loss for dense object detection," in *Proceedings of the IEEE/CVF International Conference on Computer Vision*, 2017, pp. 2980–2988.
- [20] S. Yan, C. Shen, Z. Jin, J. Huang, R. Jiang, Y. Chen, and X.-S. Hua, "Pcpl: Predicate-correlation perception learning for unbiased scene graph generation," in *Proceedings of the 28th ACM International Conference on Multimedia*, 2020, pp. 265–273.
- [21] B. Knyazev, H. de Vries, C. Cangea, G. W. Taylor, A. Courville, and E. Belilovsky, "Graph density-aware losses for novel compositions in scene graph generation," in *arXiv*, 2020.
- [22] K. Tang, Y. Niu, J. Huang, J. Shi, and H. Zhang, "Unbiased scene graph generation from biased training," in *Proceedings of the IEEE/CVF Conference on Computer Vision and Pattern Recognition*, 2020, pp. 3716–3725.
- [23] M.-J. Chiu, H. Ding, H. Yan, C. Wang, R. Zimmermann, and J. Feng, "Recovering the unbiased scene graphs from the biased ones," in *Proceedings of the 28th ACM International Conference on Multimedia*, 2021.
- [24] J. Yu, Y. Chai, Y. Hu, and Q. Wu, "Cogtree: Cognition tree loss for unbiased scene graph generation," in *International Joint Conference on Artificial Intelligence*, 2021.
- [25] Y. Guo, L. Gao, X. Wang, Y. Hu, X. Xu, X. Lu, H. T. Shen, and J. Song, "From general to specific: Informative scene graph generation via balance adjustment," in *Proceedings of the IEEE/CVF International Conference on Computer Vision*, 2021, pp. 16 383–16 392.
- [26] L. Li, L. Chen, Y. Huang, Z. Zhang, S. Zhang, and J. Xiao, "The devil is in the labels: Noisy label correction for robust scene graph generation," in *Proceedings of the IEEE/CVF Conference on Computer Vision and Pattern Recognition*, 2022, pp. 18 869–18 878.
- [27] L. Li, L. Chen, H. Shi, H. Zhang, Y. Yang, W. Liu, and J. Xiao, "Nicest: Noisy label correction and training for robust scene graph generation," *arXiv preprint arXiv:2207.13316*, 2022.
- [28] C. Lu, R. Krishna, M. Bernstein, and L. Fei-Fei, "Visual relationship detection with language priors," in *Proceedings of the European conference on computer vision (ECCV)*, 2016, pp. 852–869.
- [29] T. Furlanello, Z. Lipton, M. Tschannen, L. Itti, and A. Anandkumar, "Born again neural networks," in *International Conference on Machine Learning*. PMLR, 2018, pp. 1607–1616.
- [30] Z. Zhang and M. Sabuncu, "Self-distillation as instance-specific label smoothing," *Advances in Neural Information Processing Systems*, vol. 33, pp. 2184–2195, 2020.
- [31] L. Yuan, F. E. Tay, G. Li, T. Wang, and J. Feng, "Revisiting knowledge distillation via label smoothing regularization," in *Proceedings of the IEEE/CVF Conference on Computer Vision and Pattern Recognition*, 2020, pp. 3903–3911.
- [32] M. Tajrobekkar, K. Tang, H. Zhang, and J.-H. Lim, "Align r-cnn: A pairwise head network for visual relationship detection," *IEEE Transactions on Multimedia*, vol. 24, pp. 1266–1276, 2021.
- [33] Y. Li, X. Yang, X. Huang, Z. Ma, and C. Xu, "Zero-shot predicate prediction for scene graph parsing," *IEEE Transactions on Multimedia*, pp. 1–1, 2022.
- [34] Y. Li, W. Ouyang, X. Wang, and X. Tang, "Vip-cnn: Visual phrase guided convolutional neural network," in *Proceedings of the IEEE/CVF Conference on Computer Vision and Pattern Recognition*, 2017, pp. 1347–1356.
- [35] Y. Li, W. Ouyang, B. Zhou, J. Shi, C. Zhang, and X. Wang, "Factorizable net: an efficient subgraph-based framework for scene graph generation," in *Proceedings of the European conference on computer vision (ECCV)*, 2018, pp. 335–351.
- [36] J. Gu, H. Zhao, Z. Lin, S. Li, J. Cai, and M. Ling, "Scene graph generation with external knowledge and image reconstruction," in *Proceedings of the IEEE/CVF Conference on Computer Vision and Pattern Recognition*, 2019, pp. 1969–1978.
- [37] R. Zellers, M. Yatskar, S. Thomson, and Y. Choi, "Neural motifs: Scene graph parsing with global context," in *Proceedings of the IEEE/CVF Conference on Computer Vision and Pattern Recognition*, 2018, pp. 5831–5840.
- [38] J. Yang, J. Lu, S. Lee, D. Batra, and D. Parikh, "Graph r-cnn for scene graph generation," in *Proceedings of the European conference on computer vision (ECCV)*, 2018, pp. 670–685.
- [39] T. Chen, W. Yu, R. Chen, and L. Lin, "Knowledge-embedded routing network for scene graph generation," in *Proceedings of the IEEE/CVF Conference on Computer Vision and Pattern Recognition*, 2019, pp. 6163–6171.
- [40] K. Tang, H. Zhang, B. Wu, W. Luo, and W. Liu, "Learning to compose dynamic tree structures for visual contexts," in *Proceedings of the*

- IEEE/CVF Conference on Computer Vision and Pattern Recognition*, 2019, pp. 6619–6628.
- [41] L. Chen, H. Zhang, J. Xiao, X. He, S. Pu, and S.-F. Chang, “Counterfactual critic multi-agent training for scene graph generation,” in *Proceedings of the IEEE/CVF International Conference on Computer Vision*, 2019, pp. 4613–4623.
- [42] Q. Dong, Z. Tu, H. Liao, Y. Zhang, V. Mahadevan, and S. Soatto, “Visual relationship detection using part-and-sum transformers with composite queries,” in *Proceedings of the IEEE/CVF International Conference on Computer Vision*, 2021, pp. 3550–3559.
- [43] H. Liu, N. Yan, M. Mortazavi, and B. Bhanu, “Fully convolutional scene graph generation,” in *Proceedings of the IEEE/CVF Conference on Computer Vision and Pattern Recognition*, 2021, pp. 11 546–11 556.
- [44] I. Misra, C. Lawrence Zitnick, M. Mitchell, and R. Girshick, “Seeing through the human reporting bias: Visual classifiers from noisy human-centric labels,” in *Proceedings of the IEEE/CVF Conference on Computer Vision and Pattern Recognition*, 2016, pp. 2930–2939.
- [45] A. Desai, T.-Y. Wu, S. Tripathi, and N. Vasconcelos, “Learning of visual relations: The devil is in the tails,” in *Proceedings of the IEEE/CVF International Conference on Computer Vision*, 2021, pp. 15 404–15 413.
- [46] G. Hinton, O. Vinyals, J. Dean *et al.*, “Distilling the knowledge in a neural network,” *arXiv*, 2015.
- [47] Z. Hao, Y. Luo, Z. Wang, H. Hu, and J. An, “Cdfkd-mfs: Collaborative data-free knowledge distillation via multi-level feature sharing,” *IEEE Transactions on Multimedia*, pp. 1–13, 2022.
- [48] J. Gou, B. Yu, S. J. Maybank, and D. Tao, “Knowledge distillation: A survey,” *International journal of computer vision*, pp. 1789–1819, 2021.
- [49] L. Zhang, D. Du, C. Li, Y. Wu, and T. Luo, “Iterative knowledge distillation for automatic check-out,” *IEEE Transactions on Multimedia*, vol. 23, pp. 4158–4170, 2021.
- [50] M. Yuan and Y. Peng, “Ckd: Cross-task knowledge distillation for text-to-image synthesis,” *IEEE Transactions on Multimedia*, vol. 22, no. 8, pp. 1955–1968, 2020.
- [51] L. Chen, Y. Zheng, and J. Xiao, “Rethinking data augmentation for robust visual question answering,” in *European Conference on Computer Vision*, 2022.
- [52] X. Li, L. Chen, W. Ma, Y. Yang, and J. Xiao, “Integrating object-aware and interaction-aware knowledge for weakly supervised scene graph generation,” in *ACM International Conference on Multimedia*, 2022.
- [53] J. Yim, D. Joo, J. Bae, and J. Kim, “A gift from knowledge distillation: Fast optimization, network minimization and transfer learning,” in *Proceedings of the IEEE/CVF Conference on Computer Vision and Pattern Recognition*, 2017, pp. 4133–4141.
- [54] S. Hahn and H. Choi, “Self-knowledge distillation in natural language processing,” *arXiv preprint arXiv:1908.01851*, 2019.
- [55] S. Yun, J. Park, K. Lee, and J. Shin, “Regularizing class-wise predictions via self-knowledge distillation,” in *Proceedings of the IEEE/CVF Conference on Computer Vision and Pattern Recognition*, 2020, pp. 13 876–13 885.
- [56] K. Kim, B. Ji, D. Yoon, and S. Hwang, “Self-knowledge distillation with progressive refinement of targets,” in *Proceedings of the IEEE/CVF International Conference on Computer Vision*, 2021, pp. 6567–6576.
- [57] J. Tang, R. Shivanna, Z. Zhao, D. Lin, A. Singh, E. H. Chi, and S. Jain, “Understanding and improving knowledge distillation,” *arXiv preprint arXiv:2002.03532*, 2020.
- [58] C. Szegedy, V. Vanhoucke, S. Ioffe, J. Shlens, and Z. Wojna, “Rethinking the inception architecture for computer vision,” in *Proceedings of the IEEE/CVF Conference on Computer Vision and Pattern Recognition*, 2016, pp. 2818–2826.
- [59] B. Zoph, V. Vasudevan, J. Shlens, and Q. V. Le, “Learning transferable architectures for scalable image recognition,” in *Proceedings of the IEEE/CVF Conference on Computer Vision and Pattern Recognition*, 2018, pp. 8697–8710.
- [60] B. Guo, S. Han, X. Han, H. Huang, and T. Lu, “Label confusion learning to enhance text classification models,” *arXiv*, 2020.
- [61] T.-J. J. Wang, S. Pehlivan, and J. Laaksonen, “Tackling the unannotated: Scene graph generation with bias-reduced models,” *arXiv preprint arXiv:2008.07832*, 2020.
- [62] V. S. Chen, P. Varma, R. Krishna, M. Bernstein, C. Re, and L. Fei-Fei, “Scene graph prediction with limited labels,” in *Proceedings of the IEEE/CVF International Conference on Computer Vision*, 2019, pp. 2580–2590.
- [63] K. He, G. Gkioxari, P. Dollár, and R. Girshick, “Mask r-cnn,” in *Proceedings of the IEEE/CVF International Conference on Computer Vision*, 2017, pp. 2961–2969.
- [64] H. Zhang, Z. Kyaw, S.-F. Chang, and T.-S. Chua, “Visual translation embedding network for visual relation detection,” in *Proceedings of the IEEE/CVF Conference on Computer Vision and Pattern Recognition*, 2017, pp. 5532–5540.
- [65] Z.-S. Hung, A. Mallya, and S. Lazebnik, “Contextual translation embedding for visual relationship detection and scene graph generation,” *IEEE Transactions on Pattern Analysis and Machine Intelligence*, pp. 3820–3832, 2020.
- [66] S. Kullback and R. A. Leibler, “On information and sufficiency,” *The annals of mathematical statistics*, pp. 79–86, 1951.
- [67] T.-Y. Lin, P. Dollár, R. Girshick, K. He, B. Hariharan, and S. Belongie, “Feature pyramid networks for object detection,” in *Proceedings of the IEEE/CVF Conference on Computer Vision and Pattern Recognition*, 2017, pp. 2117–2125.
- [68] Y. Li, W. Ouyang, B. Zhou, K. Wang, and X. Wang, “Scene graph generation from objects, phrases and region captions,” in *Proceedings of the IEEE/CVF International Conference on Computer Vision*, 2017, pp. 1261–1270.
- [69] X. Wang, Y. Hua, E. Kodirov, D. A. Clifton, and N. M. Robertson, “Proselfie: Progressive self label correction for training robust deep neural networks,” in *Proceedings of the IEEE/CVF Conference on Computer Vision and Pattern Recognition*, 2021, pp. 752–761.